Ultrasensitive Telomerase Activity Detection in Circulating Tumor Cells Based on DNA Metallization and Sharp Solid-State Electrochemical Techniques

*Li Wu, Jiasi Wang, Jinsong Ren, and Xiaogang Qu**

Being considered a "liquid biopsy", circulating tumor cell (CTC) quantification is of great interest for evaluating cancer dissemination, predicting patient prognosis, and also for the evaluation of therapeutic treatments, representing a reliable potential alternative to invasive biopsies and subsequent proteomic and functional genetic analysis. Compared to a biopsy, the gold standard of current cancer diagnosis, an important characteristic of a blood test is that it is safe and can be performed at many points during the disease, allowing the development of appropriate therapy modifications and potentially improving patient's quality of life. In this work, an ultrasensitive electrochemical telomerase activity-sensing strategy is presented that utilizes DNA-templated deposition of silver nanoparticles as electroactive labels through a highly sharp solid-state Ag/AgCl reaction with DNA exonuclease III-assisted background current suppression. This nanoparticle-mediated signal amplification resulted in significantly decreased detection limit, which is better than the vast majority of reported methods and achieves a sensitivity comparable to the conventional telomeric repeat amplification protocol (TRAP). This work may pave a new PCR-free way for the detection of telomerase activity in CTCs via a noninvasive routine blood test for point-of-care diagnosis and individualized treatment of cancer.

1. Introduction

Circulating tumor cells (CTCs) are cells that have shed into the vasculature from a primary tumor or from metastasis and circulate in the bloodstream, which reflect molecular features of cells within tumor masses.[1,2] Being considered as a "liquid biopsy", CTC quantification thus is of great interest for evaluating cancer dissemination, predicting patient prognosis and also for the evaluation of therapeutic treatments, representing a reliable potential alternative to invasive biopsies and subsequent proteomic and functional genetic analysis.[3] Compared to biopsy, the gold standard of current cancer diagnosis, an important characteristic of a blood test is that it is safe and can be performed at many points during the disease, allowing development of appropriate therapy modifications and potentially improving patient's quality of life. However, convenient methods of analyzing CTCs for specific biomarkers are much less developed, which yield little phenotypic and molecular information about the CTCs.[4,5]

Finding efficient biomarkers and developing valuable profiling strategy are the standard means to further understand and exploit the use of CTCs in clinical cancer diagnosis. As a promising CTC biomarker, telomerase offers several advantages:[6–10] (a) it is a widely applicable tumor biomarker with validated diagnostic and prognostic utility in multiple cancer types; (b) it is a uniquely "functional" assay that reflects the presence of live cancer cells; (c) it can be amplified and measured accurately from small numbers of cells without the need to visualize or count the cells; (d) it can be scaled-up cheaply and rapidly to yield quantitative, operator-independent results, and; (e) such an approach would be widely applicable to nearly all solid tumor types regardless of cell sizes or surface markers on cancer cells. Therefore, telomerase activity may provide new approach for cancer diagnosis and therapy, such as inhibitors of telomerase and antisense therapy. As the telomeric repeat amplification protocol (TRAP) assay is not easily quantitated and readily contaminated by the genomic DNA and proteins in cell extract, a more definitive assessment of the role of telomerase activity in CTCs is urgent for the development of this promising field. Using PCR-free method for the accurate quantification of telomerase activity may shed light on the direct sensing of telomerase activity in CTCs and hope to shed light on the realizing of point-of-care diagnosis and individualized treatment of cancers by the noninvasive routine blood test in the future. Over the past few years, various types of PCR-free methods for direct analysis of telomerase activity have been developed.[11–19] However, due to the lack of an amplification mechanism, most do not achieve sensitivity comparable to TRAP and none of them has been used for the sensing of telomerase activity in CTCs. Therefore, a means to reliably and robustly amplify the signal and avoid

L. Wu, J. Wang, Prof. J. Ren, Prof. X. Qu
Laboratory of Chemical Biology
Division of Biological Inorganic Chemistry
State Key Laboratory of Rare Earth Resource Utilization
Changchun Institute of Applied Chemistry
University of Chinese Academy of Sciences
Chinese Academy of Sciences
Changchun, Jilin, 130022, China
E-mail: xqu@ciac.ac.cn

DOI: 10.1002/adfm.201303818

signal-to-noise interferences is essential for the application of these technologies to the rapid detection of telomerase activity present at ultralow levels from CTCs in peripheral blood.

Nanotechnology offers unique opportunities for creating highly sensitive innovative biosensing devices and ultrasensitive bioassays. The enormous signal enhancement associated with the use of nanoparticle amplifying labels and with the formation of nanoparticle–biomolecule assemblies provides the basis for ultrasensitive optical and electrical detection with PCR-like sensitivity.[20–22] DNA-templated metallization represents an efficient approach to increase the amount of the metal tracer and hence for amplifying the electrochemical response.[23,24] Inspired by these successful results, in this work, we present an ultrasensitive electrochemical telomerase activity sensing strategy that utilizes DNA-template deposition of silver nanoparticles (NPs) as electroactive labels through a highly characteristic solid-state Ag/AgCl reaction with enzyme-assisted background current-suppression. Besides that, we attempt to measure telomerase activity in CTCs using PCR-free method for the first time.

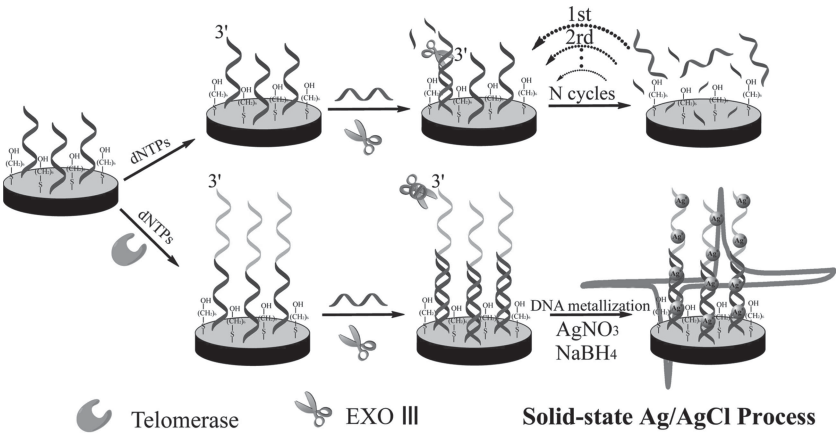

Scheme 1. Illustration of the DNA-metallization based signal amplification assay for human telomerase activity detection using enzyme-assisted background current-suppression and highly characteristic solid-state electrochemical process.

2. Results and Discussion

As shown in **Scheme 1**, the telomerase primer oligonucleotides (TS) were firstly assembled onto a clean Au electrode through Au/thiol chemistry. To ensure high hybridization efficiency, the probe density and the spatial arrangement of the probe should be optimized (Figure S1). When the electrode was placed in a solution containing telomerase and dNTPs mixture, elongation of TS occurred and more negatively charged dNTPs were introduced to the electrode surface. Since DNA is rich of phosphate groups, amino groups and heterocyclic nitrogen atoms, it offers multiple binding sites for positively charged silver ions, and these localized silver cations could be reduced to form metallic cluster that follow the contour of the DNA template.[25] Solid-state voltammetric detection of Ag nanoparticle labels has shown a major advantage in electrochemical detection due to its simplicity and uniqueness, as it involves the measurement of the signal resulting from the conversion between one surface-confined solid to another surface-confined solid.[26] The fabricated electrode was subsequently placed in 0.1 M NaCl solution with $NaNO_3$ added to maintain a sufficient electrolyte concentration for the electrochemical measurement. Two well-separated sharp current peaks were observed, which attributed to oxidation of Ag to AgCl and reduction of AgCl back to Ag, respectively (**Figure 1**). The charge efficiency for the oxidation and subsequent reduction was near 100%, suggesting reversible conversion of the Ag NPs to the silver halide phase during the anodic scan and subsequent conversion back to Ag during the cathodic scan. As it was pointed out that both the oxidized and reduced forms of the NPs are stable and sufficiently insoluble on the time scale of the experiment to prevent substantial loss of material from the NPs, which was suited for the construction of electrochemical biosensor.[27] The magnitude of the peak currents of both solid-state process depended on the extended degree of TS by telomerase, thus could be used for telomerase activity sensing. Choosing the anodic peak current (Figure 1, line a) for telomerase activity profiling, the electrochemical could be well-distinguished from background signal with a flatter baseline. Since the area underneath a voltammetric peak is proportional to the total amount of electroactive species consumed. When an equal amount of electroactive species is involved, a much larger peak current can be expected from the extremely narrow solid-state Ag/AgCl voltammetric response.[26]

Using the electrochemical impedance spectroscopy (EIS), an effective method for evaluating the interfacial electron transfer efficiency at different stages of biosensor preparation, each step can be readily detected by monitoring the electron transfer resistance (R_{et}) change, the EIS curves are shown in Figure S2. A sharp attenuation of R_{et} was observed after Exo III treated, an indicator of TS primer being successfully

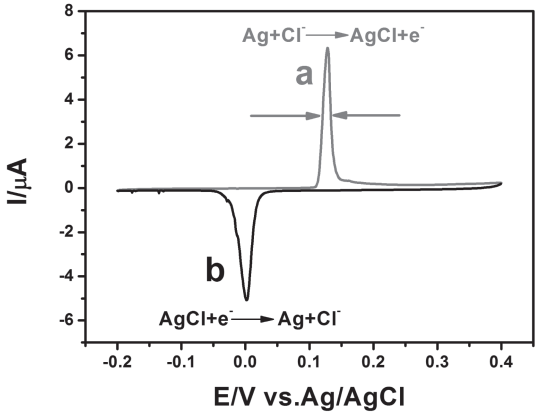

Figure 1. A typical cyclic voltammogram (CV) of silver solid-state phase transformations in N_2-saturated 0.1 M NaCl solution containing 0.1 M $NaNO_3$ as an electrolyte.

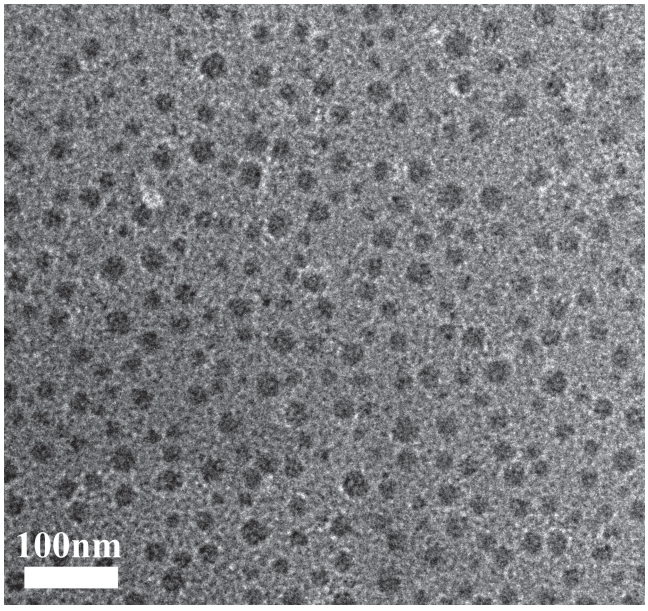

Figure 2. Transmission electron microscopy image of DNA-templated silver nanoparticles.

removed from the electrode surface. Before the sensing performance, the feasibility of silver deposition along the DNA template confined at electrode surface was first investigated by cyclic voltammetry and EIS, respectively (Figure S3). The increase of peak current in cyclic voltammograms and the decrease of R_{et} in EIS spectra demonstrate that a complete metallization of DNA has severely enhanced the conductance properties of DNA. These results are reasonable and in accordance with previous work, pointing out that DNA-templated metal deposition is an attractive approach for the self-assembly of nanoelectronics.[28–30] The transmission electron microscopy (TEM) image in **Figure 2** further provides a direct evidence of silver nanoparticles formation by this DNA-templated silver deposition strategy. This deposition process is based on selective localization of silver ions along the DNA through Ag^+/Na^+ ion exchange and formation of complexes between the silver and the DNA bases. Subsequently, the silver ion-exchanged DNA is reduced to form nanometer-sized metallic silver aggregates bound to the DNA skeleton. The ion-exchange process is highly selective and restricted to the DNA template only, which has significantly improved the sensing performance with lower nonspecific adsorption. However, it should pay attention to the fact that the TS probe itself would produce a large signal even in the absence of telomerase, which attributed to the binding of positively charged silver ions to the single strand TS probes and subsequently produced a measurable electrochemical signal.

In electrochemical detection, as in many analytical methods, the signal-to-noise ratio is crucial for the success of the experiment. Ideally, there should be no current at the resting level and a large increase in the peak current should be observed after manipulation of the sample.[31] This scenario is, to a certain extent, achieved when background suppression strategy is used. Enzyme-assisted background current-suppression was chosen at present because of the comparatively reduced background signal resulting from the remove of non-reacted TS from the electrode surface. In this method, exonuclease III (Exo III), the nuclease which specifically cleaves duplex DNA from blunt or recessed 3′-termini,[32] was used to reduce the blank peak current generated by TS primer and improved the biosensor's performance by the nuclease assisted TS primer strand-cleavage cycle. As illustrated in Scheme 1, when TS primer was challenged with its complementary strand, the hybridization led the TS primer to have a blunt 3′-terminus. Exo III then could catalyze the stepwise removal of mononucleotides from this terminus, releasing the complementary DNA and ultimately the cleavage products of TS primer could be removed from the surface by washing with buffered solution. During the hydrolysis process, the released complementary DNA is free to bind to another primer on electrode surface to trigger a new hydrolysis reaction, leading to complete removing of unextended primer. Consequently, almost neglectable peak current was obtained from the Exo III treated TS primer modified electrode (**Figure 3**), suppressing the background signal. Once extended by the telomerase, the blunt 3′-terminus of the duplex formed by TS primer and its complementary strand changed to the 3′-protruding, deforming the Exo III recognition site. The endonuclease cannot cleave the probe sequence in this case. Thus, the high electrochemical signal is observed, indicating a signal-on signaling scheme that is preferable to a signal-off one. Additionally, a striking high-signal-to-noise ratio is also achieved, which is predicted to offer an attractive analytical performance.

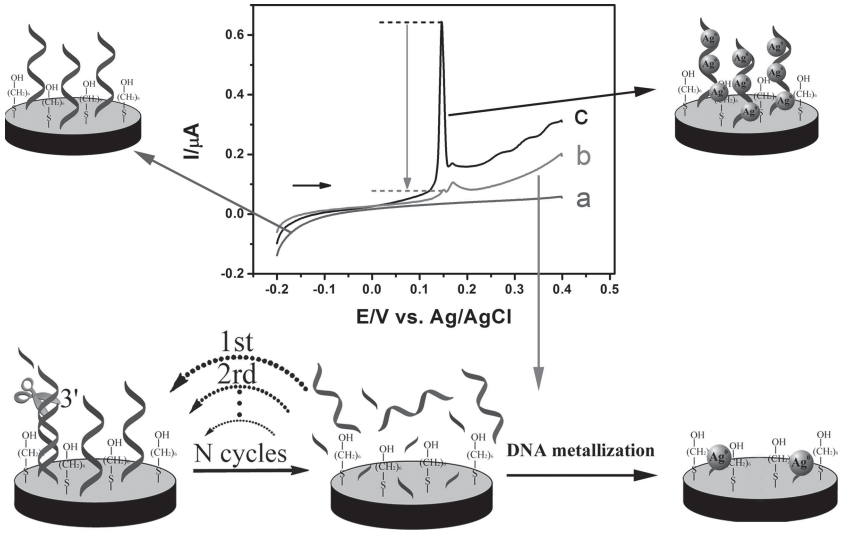

Figure 3. The voltammetric responses of different modified Au electrode in N_2-saturated 0.1 M NaCl solution containing 0.1 M $NaNO_3$ as an electrolyte: TS and MCH mixed monolayer without (a) and with (c) silver deposition; TS and MCH modified electrode pretreated by EXO III-assisted TS primer strand-cleavage cycle with silver deposition (b). Scan rate: 10 mV/s.

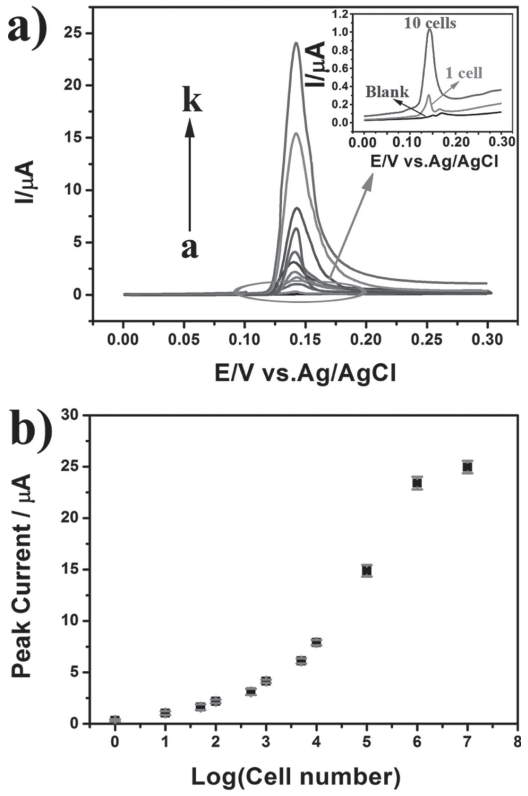

Figure 4. a) The voltammetric responses of silver nanoparticles grown along the TS template extended by telomerase extracted from different number of MCF-7 cell: (a) blank (b) 1 cell; (c) 10 cells; (d) 50 cells; (e) 100 cells; (f) 500 cells; (g) 1×10^3 cells; (h) 5×10^3 cells; (i) 1×10^4 cells; (j) 1×10^5 cells; (k) 1×10^6 cells. Inset shows the voltammetric response of the telomerase biosensor at lower cell number. b) Dependence of the peak current of the anodic Ag/AgCl solid-state process on the amount of cancer cells.

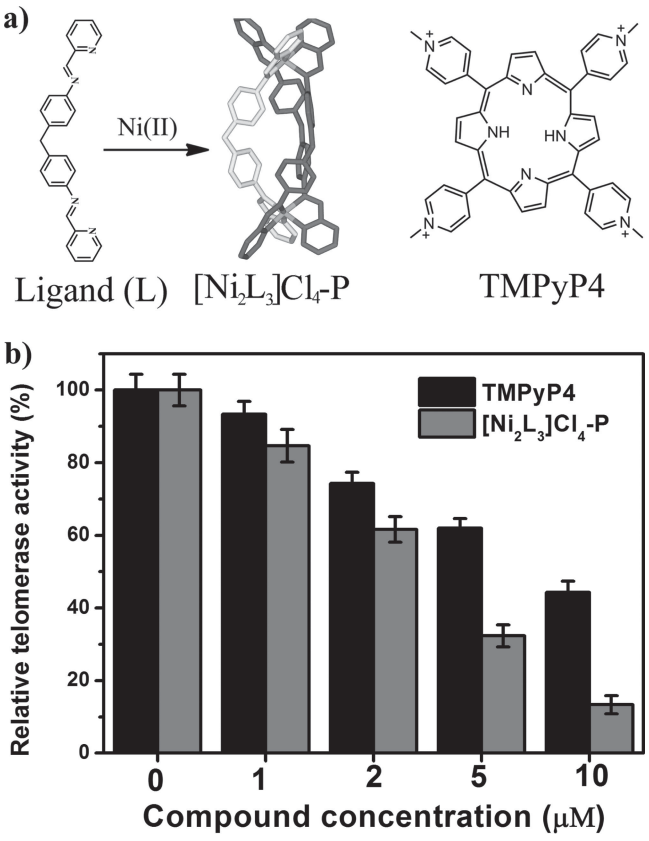

Figure 5. Inhibition of telomerase activity by G-quadruplex ligand TMPyP4, $[Ni_2L_3]Cl_4$-P with solid-state electrochemical assay. The telomerase activity equivalent to 1000 MCF-7 cells in the presence of increasing concentrations of G-quadruplex ligand was represented by anodic peak current and normalized.

The constructed biosensor showed a good response to telomerase activity over a wide cancer cell numbers range (**Figure 4**). The peak current increased when the cell amount was increased from 1 cell to 1×10^6 cells. The current then approached a plateau when the cell number was further increased. Furthermore, even when the telomerase activity equivalent to a single MCF-7 cancer cell was present, the signal detected was still well distinguished (Figure 4a, inset), which achieved the sensitivity comparable to TRAP.[33] Using DNA-metallization method and highly characteristic solid-state electrochemical process for nanoparticle-mediated signal amplification resulted in significantly decreased detection limit, which was better than the vast majority of reported methods[11,13,34–36] (Table S1) and comparable to the most recently reported exponential isothermal amplification of telomerase repeat assay.[37]

Optimal telomerase activity requires an unfolded single-stranded telomeric overhang. Folding of telomeric DNA into G-quadruplex structure can influence the extent of telomere elongation in vitro and may therefore act as a negative regulator of elongation in vivo.[38] Therefore, ligands that selectively bind to and stabilize telomeric G-quadruplex structures can act as telomerase inhibitors. Here a metallo-supramolecular cylinder $[Ni_2L_3]Cl_4$-P(L = $C_{25}H_{20}N_4$) and a cationic porphyrin tetra-(*N*-methyl-4-pyridyl) porphyrin (TMPyP4) (**Figure 5**a), which had been proved to inhibit telomerase activity by TRAP assay,[39,40] were selected to evaluate our electrochemical assay. As shown in Figure 5b, $[Ni_2L_3]Cl_4$-P had a stronger inhibitory effect on telomerase than TMPyP4. The IC_{50} values for two compounds detected by the developed ultrasensitive PCR-free electrochemical method were 3137 nM for $[Ni_2L_3]Cl_4$-P and 7270 nM for TMPyP4, respectively, the results were more reliable than TRAP assay.[41] These results indicate that the developed electrocatalytic assay for telomerase detection may be used for initial screening of G-quadruplex binding agents and telomerase inhibitors.

Telomerase is a unique enzyme that it is a reverse transcriptase endogenous to human cells and requires an internal RNA component to work as a template. The addition of telomerase repeats (TTAGGG) to a known telomerase primer was sensitive to heat, which is known to destroy the essential RNA template and reverse transcriptase protein of telomerase.[11,12] When MCF-7 cell extract was pretreated by heat, an obvious decrease of relative telomerase activity was detected (Figure S4). Moreover, to demonstrate that it is a general and reliable method for telomerase detection, other cancer cell line MDA-MB-231, HeLa, K562, HepG2 and a normal cell line

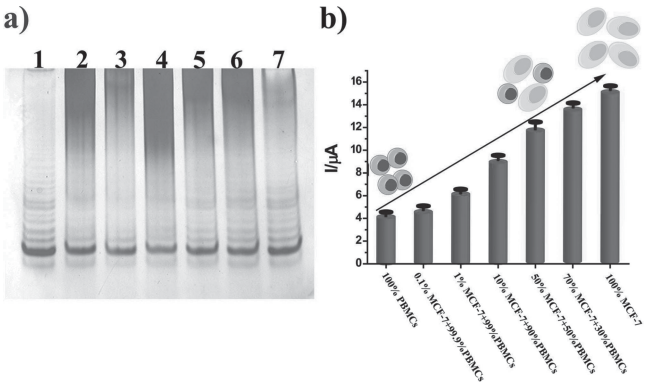

Figure 6. a) Quantitation of TRAP products obtained with MCF-7 cell and artificial CTCs extract. Lane 1: the control band of MCF-7; lane 2: PBMCs from healthy donor; lanes 3–7: mixed suspensions of MCF-7 and PBMCs at different MCF-7/PBMCs ratios: 1:999 (lane 3); 1:99 (lane 4); 10:90 (lane 5); 50:50 (lane 6); 70:30 (lane 7). The entire total cells amount was equivalent to 1×10^5. b) Electrochemical results obtained for mixed suspensions of MCF-7 and PBMCs at different MCF-7/ PBMCs ratios.

HUVEC were tested. The telomerase activity of each cell line was normalized to the activity of MCF-7 cell. As expected, the tests on HUVEC cell did not generate any electrochemical signal due to the lack of telomerase activity in normal cells; whereas the other five cancer cell lines showed positive telomerase activity (Figure S4).

Inspired by the above successful results, the optimized process was used for electrochemical sensing of telomerase activity in CTCs using breast cancer cells (MCF-7) as a model. CTCs circulate in the blood flow among thousands of other human cells, thus we chose peripheral blood mononuclear cells (PBMCs) to simulate the possible interference caused by other cells in our detection. The artificial CTCs samples were prepared by mixing in suspension the MCF-7 cells with PBMCs in different proportions according to the previous report.[42–44] As shown in **Figure 6**a, the results obtained with the TRAP assay correlated with those obtained with electrochemical method at the higher MCF-7/PBMCs level. However, at the lower MCF-7/PBMCs ratio, the TRAP assay has no effect to sense the telomerase activity of MCF-7 in the mixture (lane 2–4). Additionally, the existence of abundant genomic DNA and proteins in PBMCs also interfere the detection (Figure 6a, black region in lanes 2–7). Compared to TRAP assay, the PCR-free electrochemical method developed here is more reliable to quantify the telomerase activity and also has a good performance at lower MCF-7/PBMCs (Figure 6b). A certain amount of electrochemical signal was obtained from the sample containing 100% of PBMCs. The increasing percentage of MCF-7 cells assayed in the presence of decreasing quantities of PBMCs resulted in an increase in the analytical signal, demonstrating the specificity of the assay.

3. Conclusions

We have developed a PCR-free electrochemical method for telomerase activity sensing based on DNA metallization using highly characteristic solid-state electrochemical process. This assay has been demonstrated to be applicable for the initial screening of telomerase inhibitors as anticancer drug agents. More importantly, since the conventional TRAP method is time consuming, complicated, not easily quantitated and not proper to be carried out in complicated analysis system, the present assay is PCR-free, simple in design, easy to quantify and avoids PCR amplification or contaminants-related errors, which makes it more reliable to evaluate telomerase activity in CTCs. Although it is at preliminary stage for telomerase activity sensing in CTCs and using them for providing information in clinical cancer therapy, the clinical and pathophysiological significance of CTCs will encourage the scientists to devote much effort in this field. The work presented here paves a new way for telomerase activity measuring in CTCs with PCR-free method, hoping to realize point-of-care diagnosis and individualized treatment of cancers by the noninvasive routine blood test in the future.

4. Experimental Section

Materials: The dNTPs (dATP, dGTP, dCTP and dTTP mixture), exonuclease III and the oligonucleotide used in this paper were offered by Biotechnology Inc. (Shanghai, PR China). The sequence was as following: TS primer: 5′-HS$(CH_2)_6$TTTTTTTTTAATCCGTCGAGCAGA GTT-3′; TS primer complementary strand: 5′-AAC TCT GCT CGA CGG ATT AAA AAAAAAAAA AAA-3′. Silver nitrate ($AgNO_3$) and sodium borohydride ($NaBH_4$) were purchased from Alfa Aesar. All other reagents were of analytical reagent grade, and used as received. All aqueous solutions were prepared with nanopure water (18.2 MΩ cm, Milli-Q, Millipore).

Apparatus and Characterization: Transmission electron microscopic (TEM) images were recorded using a FEI TECNAI G2 20 high-resolution transmission electron microscope operating at 200 kV. Circular dichroism (CD) spectra was carried out on a JASCO J-810 spectropolarimeter equipped with a temperature controlled water bath. The optical chamber of CD spectrometer was deoxygenated with dry purified nitrogen (99.99%) for 45 min before use and kept the nitrogen atmosphere during experiments. Electrochemical measurements were performed with a CHI 660B Electrochemistry Workstation (CHI, USA). A three-electrode setup was used with a common Ag/AgCl reference and a Pt wire auxiliary electrodes placed in the cencral buffer solution. Cyclic voltammetry (CV) data for conductivity characterization were collected at 100 mV/s in 10 mM $K_3[Fe(CN)_6]$, 1 M KCl and 100 mM PBS (pH 7.5) unless otherwise indicated. EIS was performed using CHI 660B in 100 mM PBS containing 10 mM $K_3[Fe(CN)_6]/K_4[Fe(CN)_6]$ (1:1) mixture with 1 M KCl as the supporting electrolyte. The impedance spectra were recorded within the frequency range of 10^{-2}–10^5 Hz. The amplitude of the applied sine wave potential in each case was 5 mV.

Synthesis and Characterization of Metallo-supramolecular Complex: The metallo-supramolecular cylinder $[Ni_2L_3]Cl_4$ was synthesized and purified according to the previous report.[39] In the methods, $[Ni_2L_3]PF_6$ salt was only used to characterize the purities and structures of the compounds. The purity was determined by ESI-MS and elemental analysis. Electrospray ionization mass spectra were recorded on a Finnigan LCQ ion trap mass spectrometer (ThermoFinnigan, San Jose, CA, USA). Element analysis was carried out on Elementar Aanlysensysteme GmbH Vario EL (HAMAU, Germany). $[Ni_2L_3](PF_6)_4$, ESI-MS (CH_3CN): m/z 311.7 ($[Ni_2L_3]^{4+}$); elemental analysis: calculated percentage: C, 49.27; H, 3.29; N, 9.20; found percentage: C, 49.48; H, 3.32; N, 9.17. The $[Ni_2L_3]Cl_4$ were obtained by anion metathesis in acetonitrile using tetrabutylammonium chloride. The enantiomerically pure $[Ni_2L_3]Cl_4$ was obtained by using a cellulose (~20 μ, Aldrich) column and eluting with 20 mM NaCl aqueous solution. UV-vis spectroscopy was used to determine the concentration of enantiomer and CD spectra of the two enantiomers prepared at the

same concentration were used to estimate their purity (Figure S5). The samples of purified Ni-M and Ni-P enantiomer were collected and freeze-dried for future use.

Isolation of Human Peripheral Blood Mononuclear Cells (PBMCs): Human peripheral blood mononuclear cells were isolated by Ficoll-Hypaque gradient centrifugation.[42] Whole blood from healthy individual volunteers was collected into sterile heparinized vacutainer tubes. Equal volumes of blood and PBS were mixed gently with a sterile pipette in a 50 mL test tube. This blood-PBS mixture was slowly overlaid on to 15 mL of Ficoll-Hypaque solution. It was then centrifuged at 1500 rpm for 40 min at 18 °C. The upper layer containing plasma and platelets was removed with a sterile pipette. The buff-coloured layer containing PBMCs was transferred into a fresh tube, washed twice with 20 mL PBS and resuspended into RPMI complete media. Cells were counted and the viability of the cells was determined by trypan blue exclusion test.

Cell Culture and Telomerase Extraction: Briefly, various cell lines were cultured in DMEM medium supplemented with 10% fetal calf serum, and the cells were maintained at 37 °C in a humidified atmosphere (95% air and 5% CO_2). Cells (For extraction of telomerase from CTCs model, artificial CTC samples were prepared by spiking PBMCs with MCF-7 cells at specific ratios) were collected in the exponential phase of growth, and 1×10^6 cells were dispensed in a 1.5 mL EP tube, washed twice with ice-cold phosphate buffered saline (PBS) solution, and resuspended in 100 µL of ice-cold CHAPS lysis buffer (10 mM Tris-HCl, pH 7.5, 1 mM $MgCl_2$, 1 mM EGTA, 0.1 mM PMSF, 5 mM mercapto ethanol, 0.5% CHAPS, 10% glycerol). The CHAPS lysis buffer was pretreated with RNA secure according to the manufacturer's instructions. The lysate was incubated for 30 min on ice and centrifuged 20 min at 12 000 rpm, 4 °C, to pellet insoluble material. Without disturbing the pellet, carefully transfer the cleared lysate to a fresh 1.5 mL EP tube. The lysate was used immediately for telomerase assay or frozen at –80 °C.

Electrochemical Detection of Telomerase: The gold disk electrodes (Φ = 2 mm, CH Instruments, Austin, TX) were prepared by polishing with 0.3 and 0.05 µm deagglomerated γ alumina (BUEHLER, UAS) suspensions followed by sonication in water and multiple steps of electrochemical cleaning steps (a series of oxidation and reduction cycling in 0.5 M NaOH, 0.5 M H_2SO_4, 0.01 M KCl/0.1 M H_2SO_4, and 0.05 M H_2SO_4)[45] before modification with the thiolated TS probe. For the samples analysis, different concentration of thiolated TS primer was pretreated with 10 mM TCEP in buffer (10 mM Tris-HCl, 1 mM EDTA, 0.1 M NaCl, pH 7.4) for 30 min. Then a 10-µL of TS primer was added on the functionalized electrode surface and kept under humidity for 12 h at room temperature. Subsequently, the modified surface was rinsed with buffer solution and following passivated with MCH in tris buffer for 30 min. After being washed with 10 mM Tris-HCl (pH 8.3) buffer solution for several seconds, the electrode was dried in a dry nitrogen gas and stored in air prior to use.

For telomerase extension reaction, telomerase extracts were diluted in lysis buffer with respective number of cells; the extracts (10 µL) were added into the RNA secure pretreated extension solution containing 1×TRAP buffer, (20 mM Tris-HCl pH 8.3, 1.5 mM $MgCl_2$, 63 mM KCl, 0.005% Tween 20, 1 mM EGTA, BSA 0.1 mg/mL) and 2 mM dNTP mix. (For inhibition of telomerase by G-quadruplex ligands, indicated $[Ni_2L_3]Cl_4$-P and 5,10,15,20-tetra(*N*-methyl-4-pyridyl) porphine (TMPyP4) was mixed with telomerase extract equivalent to 1000 MCF-7 cells. For negative controls, telomerase extracts were heat-treated at 95 °C for 10 min). 20 µL of a reaction solution prepared above was placed on the TS primer functionalized electrode and incubated at 37 °C for 1h to allow the extention reaction by telomerase to proceed. After extention reaction by telomerase, the electrode should be rinsed with a 0.2 M acetate buffer solution (pH 4.8). After hybridized with the TS primer complementary strand, the working electrode was allowed to be washed with buffer. Subsequently, 20 µL of endonuclease solution containing 2 U/mL Exo III was placed onto the resulting electrode surface and incubated at 37 °C for 60 min. The surface was then washed by Tris-HCl buffer (20 mM, pH 8.3) and stored in air prior to use.

For electrochemical detection, the modified electrodes were prior immersed in 100 µM $AgNO_3$ in buffer (20 mM HEPES, 100 mM $NaNO_3$, pH 7.4) for 1h and following washed with buffer. Subsequently, the modified electrode were dipped into a freshly prepared $NaBH_4$ (10 mM in HEPES buffer) for 10 min and washed with buffer. The electrode was then placed in a 0.1 M NaCl solution with 0.1 M $NaNO_3$ as an electrolyte for the electrochemical measurement from –0.2 V to 0.4 V versus a Ag/AgCl (3 M KCl) reference electrode.

For TEM characterization, the above modified electrodes were immersed in distilled water and sonicated to collect the silver nanoparticles. Following, the sample was dropped on the copper mesh and stored in air prior to use.

Supporting Information

Supporting Information is available from the Wiley Online Library or from the author.

Acknowledgements

This work was supported by 973 Project (2011CB936004,2012CB720602), and NSFC (21210002, 91213302).

Received: November 11, 2013
Revised: December 10, 2013
Published online: January 23, 2014

[1] K. Pantel, C. Alix-Panabieres, *Trends Mol. Med.* **2010**, *16*, 398.
[2] K. Pantel, R. H. Brakenhoff, *Nat. Rev. Cancer* **2004**, *4*, 448.
[3] K. Pantel, R. H. Brakenhoff, B. Brandt, *Nat. Rev. Cancer* **2008**, *8*, 329.
[4] M. Yu, S. Stott, M. Toner, S. Maheswaran, D. A. Haber, *J. Cell Biol.* **2011**, *192*, 373.
[5] J. den Toonder, *Lab Chip* **2011**, *11*, 375.
[6] T. Xu, B. Lu, Y.-C. Tai, A. Goldkorn, *Cancer Res.* **2010**, *70*, 6420.
[7] L. R. Gauthier, C. Granotier, J. C. Soria, S. Faivre, V. Boige, E. Raymond, F. D. Boussin, *Brit. J. Cancer* **2001**, *84*, 631.
[8] J. C. Soria, L. Morat, C. Durdux, M. Housset, A. Cortez, R. Blaise, L. Sabatier, *J. Urol.* **2002**, *167*, 352.
[9] J. C. Soria, L. R. Gauthier, E. Raymond, C. Granotier, L. Morat, J. P. Armand, F. D. Boussin, L. Sabatier, *Clin. Cancer Res.* **1999**, *5*, 971.
[10] K. Fizazi, L. Morat, L. Chauveinc, D. Prapotnich, R. De Crevoisier, B. Escudier, X. Cathelineau, F. Rozet, G. Vallancien, L. Sabatier, J. C. Soria, *Ann. Oncol.* **2007**, *18*, 518.
[11] J. Wang, L. Wu, J. Ren, X. Qu, *Small* **2012**, *8*, 259.
[12] L. Wu, J. Wang, L. Feng, J. Ren, W. Wei, X. Qu, *Adv. Mater.* **2012**, *24*, 2447.
[13] Y. Xiao, V. Pavlov, T. Niazov, A. Dishon, M. Kotler, I. Willner, *J. Am. Chem. Soc.* **2004**, *126*, 7430.
[14] T. Niazov, V. Pavlov, Y. Xiao, R. Gill, I. Willner, *Nano Lett.* **2004**, *4*, 1683.
[15] W. Q. Yang, X. Zhu, Q. D. Liu, Z. Y. Lin, B. Qiu, G. N. Chen, *Chem. Commun.* **2011**, *47*, 3129.
[16] Z. Y. Shao, Y. X. Liu, H. Xiao, G. X. Li, *Electrochem. Commun.* **2008**, *10*, 1502.
[17] Y. Weizmann, F. Patolsky, O. Lioubashevski, I. Willner, *J. Am. Chem. Soc.* **2004**, *126*, 1073.
[18] M. Gabourdes, *Anal. Biochem.* **2004**, *333*, 105.
[19] R. C. Qian, L. Ding, H. X. Ju, *J. Am. Chem. Soc.* **2013**, *135*, 13282.

[20] H. Wang, R. H. Yang, L. Yang, W. H. Tan, *ACS Nano* **2009**, *3*, 2451.
[21] S. P. Song, Y. Qin, Y. He, Q. Huang, C. H. Fan, H. Y. Chen, *Chem. Soc. Rev.* **2010**, *39*, 4234.
[22] J. Wang, *Small* **2005**, *1*, 1036.
[23] J. Wang, O. Rincon, R. Polsky, E. Dominguez, *Electrochem. Commun.* **2003**, *5*, 83.
[24] S. Hwang, E. Kim, J. Kwak, *Anal. Chem.* **2004**, *77*, 579.
[25] Y. Lin, Y. Tao, F. Pu, J. Ren, X. Qu, *Adv. Funct. Mater.* **2011**, *21*, 4565.
[26] J. Zhang, B. P. Ting, N. R. Jana, Z. Gao, J. Y. Ying, *Small* **2009**, *5*, 1414.
[27] P. Singh, K. L. Parent, D. A. Buttry, *J. Am. Chem. Soc.* **2012**, *134*, 5610.
[28] J. Liu, Y. Geng, E. Pound, S. Gyawali, J. R. Ashton, J. Hickey, A. T. Woolley, J. N. Harb, *ACS Nano* **2011**, *5*, 2240.
[29] E. Braun, Y. Eichen, U. Sivan, G. Ben-Yoseph, *Nature* **1998**, *391*, 775.
[30] H. A. Becerril, R. M. Stoltenberg, D. R. Wheeler, R. C. Davis, J. N. Harb, A. T. Woolley, *J. Am. Chem. Soc.* **2005**, *127*, 2828.
[31] S. Zhang, R. Hu, P. Hu, Z.-S. Wu, G.-L. Shen, R.-Q. Yu, *Nucleic Acids Res.* **2010**, *38*, e185.
[32] C. Zhao, L. Wu, J. Ren, X. Qu, *Chem. Commun.* **2011**, *47*, 5461.
[33] N. W. Kim, F. Wu, *Nucleic Acids Res.* **1997**, *25*, 2595.
[34] G. Zheng, W. L. Daniel, C. A. Mirkin, *J. Am. Chem. Soc.* **2008**, *130*, 9644.
[35] S. Sato, H. Kondo, T. Nojima, S. Takenaka, *Anal. Chem.* **2005**, *77*, 7304.
[36] X. Zhou, D. Xing, D. Zhu, L. Jia, *Anal. Chem.* **2009**, *81*, 255.
[37] L. Tian, Y. Weizmann, *J.Am. Chem. Soc.* **2012**, *135*, 1661.
[38] A. M. Zahler, J. R. Williamson, T. R. Cech, D. M. Prescott, *Nature* **1991**, *350*, 718.
[39] H. J. Yu, X. H. Wang, M. L. Fu, J. S. Ren, X. G. Qu, *Nucleic Acids Res.* **2008**, *36*, 5695.
[40] H. Han, D. R. Langley, A. Rangan, L. H. Hurley, *J. Am. Chem. Soc.* **2001**, *123*, 8902.
[41] A. De Cian, G. Cristofari, P. Reichenbach, E. De Lemos, D. Monchaud, M.-P. Teulade-Fichou, K. Shin-ya, L. Lacroix, J. Lingner, J.-L. Mergny, *Proc. Natl. Acad. Sci. USA* **2007**, *104*, 17347.
[42] S. S. Banerjee, A. Jalota-Badhwar, S. D. Satavalekar, S. G. Bhansali, N. D. Aher, R. R. Mascarenhas, D. Paul, S. Sharma, J. J. Khandare, *Adv. Healthcare Mater.* **2013**, *2*, 800.
[43] W. Chen, S. Weng, F. Zhang, S. Allen, X. Li, L. Bao, R. H. W. Lam, J. A. Macoska, S. D. Merajver, J. Fu, *ACS Nano* **2013**, *7*, 566.
[44] M. Maltez-da Costa, A. de la Escosura-Muñiz, C. Nogués, L. Barrios, E. Ibáñez, A. Merkoçi, *Nano Lett.* **2012**, *12*, 4164.
[45] Y. Peng, X. Wang, Y. Xiao, L. Feng, C. Zhao, J. Ren, X. Qu, *J. Am. Chem. Soc.* **2009**, *131*, 13813.